Pharmaceutical Research, Vol. 7, No. 4, 1990

Research Article

Transepithelial Transport of Aliphatic Carboxylic Acids Studied in Madin Darby Canine Kidney (MDCK) Cell Monolayers

Moo J. Cho,[1,4] Anthony Adson,[2] and F. J. Kezdy[3]

Received July 27, 1989; accepted October 17, 1989

Transport of ^{14}C-labeled acetic, propionic (PA), butyric, valeric, heptanoic (HA), and octanoic (OA) acids across the Madin Darby canine kidney (MDCK) epithelial cell monolayer grown on a porous polycarbonate membrane was studied in Hanks' balanced salt solution (HBSS) at 37°C in both apical-to-basolateral and basolateral-to-apical directions. At micromolar concentrations of solutes, metabolic decomposition was significant as evidenced by $[^{14}C]CO_2$ production during the OA transport. The apparent permeability (Pe) indicates that as lipophilicity increases, diffusion across the "unstirred" boundary layer becomes rate limiting. In support of this notion, transport of OA and HA was enhanced by agitation, showed an activation energy of 3.7 kcal/mol for OA, and resulted in identical Pe values for both transport directions. Analysis of Pe changes with varying alkyl chain length resulted in a ΔG of -0.68 ± 0.09 kcal/mol for $-CH_2$-group transfer from an aqueous phase to the MDCK cells. When the intercellular tight junctions were opened by the divalent chelator EGTA in Ca^{2+}/Mg^{2+}-free HBSS, transport of the fluid-phase marker Lucifer yellow greatly increased because of paracellular leakage. PA transport also showed a significant increase, but OA transport was independent of EGTA. Although albumin also undergoes paracellular transport in the presence of EGTA and OA binds strongly to albumin, OA transport in EGTA solution was unchanged by albumin. These observations indicate that transmembrane transport is the major mechanism for lipophilic substances. The present study, together with earlier work on the transport of polar substances, shows that the MDCK cell monolayer is an excellent model of the transepithelial transport barrier.

KEY WORDS: transepithelial transport; model cellular transport barrier; Madin Darby canine kidney (MDCK) cell monolayer; aliphatic acids.

INTRODUCTION

Structural requirements for optimal *in vivo* transport are important factors in the development of new therapeutic agents. Favorable biological activity of a drug candidate cannot be exploited unless the new entity is bioavailable via the intended route of administration, e.g., peroral. Thus, it is important to develop convenient and rapid methods for assessing the transepithelial mobility of new chemical entities. We have tested the Madin Darby canine kidney (MDCK)[5] epithelial cell monolayer as a potential model system. Briefly, MDCK cell monolayers are grown on a polycarbonate membrane with 3-μm pores. The membrane, 2.45 cm in diameter, is part of a commercially obtained presterilized culture insert which provides two chambers when placed in a regular six-well cell culture plate. In effect, this commercial system resembles a diffusion cell or an Ussing chamber. In our previous study (1), an attempt was made to characterize the system by investigating the transport of polar fluid-phase markers such as sucrose, Lucifer yellow CH (LY), inulin, and dextran. For these types of substances, leakage through the intercellular junctional/lateral space (paracellular shunt pathway) should be the dominant route. With these permeants a flux-rate ratio normalized to a standard permeant was used for comparing transepithelial mobility (1). As part of an ongoing effort to characterize the system further, we have now investigated the transport of acetic (AA), propionic (PA), butyric (BA), valeric (VA), heptanoic (HA), and octanoic (OA) acids.

Aliphatic carboxylic acids were chosen as probes for the following reasons. (a) Their transport across the intestinal (2) and buccal epithelia (3) has been a subject of investigation for some time. (b) Their binding to albumin is well docu-

[1] Drug Delivery Systems Research, The Upjohn Company, Kalamazoo, Michigan 49001.

[2] Present address: Pharmaceutical Chemistry Department, The University of Kansas, Lawrence, Kansas 66045-2504.

[3] Biopolymer Research, The Upjohn Company, Kalamazoo, Michigan 49001.

[4] To whom correspondence should be addressed.

[5] Abbreviations used: AA, acetic acid; BA, butyric acid; BSA, bovine serum albumin; EGTA, [ethylene bis(oxyethylenenitrilo)]-tetraacetic acid; HA, heptanoic acid; HBSS, Hanks' balanced salt solution; HSA, human serum albumin; LY, Lucifer yellow CH; MDCK, Madin Darby canine kidney; OA, octanoic acid; PA, propionic acid; VA, valeric (pentanoic) acid.

0724-8741/90/0400-0325$06.00/0

mented (4). (c) Their biochemical fate during and subsequent to cellular uptake is also well characterized, especially their β-oxidative catabolism (5). (d) Finally, radiolabeled carboxylic acids are readily available, offering easy determinations with a high sensitivity.

In addition to assessing the effect of systematic changes in chain length and, hence, lipophilicity on transport across the MDCK cell monolayer, we also determined the effect of opening the tight junction (6) on transport. The results further clarify the contribution of paracellular transport to the overall flux.

MATERIALS AND METHODS

Materials

Radiolabeled carboxylic acid sodium salts were obtained commercially and used without further purification: AA, PA, BA, and OA were from New England Nuclear (Boston, MA), whereas VA and HA were from Sigma (St. Louis, MO). In all cases, the carbonyl carbon was labeled with ^{14}C. For convenience, stock solutions of 0.1 m*M* were prepared in Hanks' balanced salt solution (HBSS) and stored at −10°C until used. Cold AA was obtained from Mallinckrodt (Paris, KY), PA, VA, and HA were from Aldrich (Milwaukee, WI), BA sodium salt was from Sigma, and OA was from Eastman (Rochester, NY). Materials used in cell culture were the same as in our previous study (1). Iodinated bovine serum albumin ([^{125}I]BSA) was purchased from New England Nuclear. Fragments smaller than MW 30,000 and free $^{125}I_2$ were eliminated by means of Centricon 30 (Amicon, Danvers, MA). These impurities accounted for approximately 3% of the radioactivity. Iodinated BSA was used only in assessing the permeability of human serum albumin (HSA). All transport experiments which were carried out in the presence of albumin used HSA. LY was obtained from Molecular Probes (Eugene, OR) and used without further purification. [Ethylene bis(oxyethylenenitrilo)]tetraacetic acid (EGTA) was obtained from Eastman. Fatty acid-free HSA was purchased from Miles Laboratories (Naperville, IL).

MDCK Cell Monolayer

Cell monolayers were prepared as described (1) with the following modifications. The final cell suspension for seeding was in the culture medium at a concentration 2.4×10^5 cells/ml. When 1.5 ml of this suspension is added to a 2.45-cm Transwell (Costar, Cambridge, MA), it provides a seeding concentration of 7.5×10^4 cells/cm^2. Previously, we prepared the cell suspension in HBSS such that 0.1 ml contained a sufficient number of cells for a given seeding density. The culture medium used in the present study did not contain 20 m*M* *N*-2-hydroxyethylpiperazine-*N*-2-ethanesulfonic acid, although it was still added to the HBSS used. Other routine procedures, such as measurement of transepithelial electrical resistance, were the same as before (1).

Transport Experiments

Cell confluence was generally achieved on day 4, as indicated by a relatively constant electrical resistance of approximately 210 Ω · cm^2. In our experiments the cells were used within 2 days after reaching confluence. The nutrient-rich culture medium was replaced with HBSS at 37°C, 60 min before a transport experiment began. Apical-to-basal transport was initiated by replacing the 1.5-ml of HBSS with the same volume of HBSS containing a carboxylic acid. At 30- or 60-min intervals, the Transwell was simply moved to a new well in a six-well culture plate containing 2.6 ml of fresh HBSS at 37°C. The appearance of radioactivity in the basal side was determined for ^{14}C with a Packard Model Tri-Carb 4640 liquid scintillation counter (Packard, Downers Grove, IL) and for [^{125}I]BSA using a Packard Model Auto-Gamma 5650 gamma counter. In all cases, the radioactivity was determined in triplicate.

Basal-to-apical transport was monitored by measuring the appearance of radioactivity in 1.5 ml HBSS withdrawn from Transwell after 2.6 ml HBSS containing a carboxylic acid had been introduced to a well. The Transwell was immediately refilled with 1.5 ml fresh HBSS. When agitation of the system was desired, the six-well plate was continuously stirred on an Adams Nutator Model 1105 cell rocker (Clay Adams, Parsippany, NJ). The rocking motion was briefly interrupted for sampling. All transport experiments used at least two cell monolayers for a given test permeant. Once an experimental protocol was established, it became rather routine to use as many as 24 cell monolayers in one series of transport experiments.

Radioactivity retained in the cell layer during or after a transport experiment was determined as follows. After the HBSS in a Transwell was completely withdrawn, the cell layer was briefly washed by immersion in a beakerful of cold saline (ca. 250 ml). It was then allowed to dry at room temperature. The cell layer plus polycarbonate membrane was cut out with a scalpel and placed in a liquid scintillation vial. To this was added 0.4 ml water for hydration. Approximately 30 min later, 1.0 ml of Protosol (New England Nuclear) was added to dissolve both cells and the synthetic membrane. After overnight in the dark at room temperature, 10 ml of a scintillation cocktail was added and radioactivity was determined as described above.

RESULTS AND DISCUSSION

Permeability Analysis

In the absence of an active transport system, movement of drug molecules in various tissues and organs is driven by a difference in chemical potential, i.e., a concentration gradient. In the present study, mass transport at a given time is expressed in terms of mass (mol) · area^{-1} (cm^{-2}) · initial concentration^{-1} (L/mol), or L/cm^2. When it is plotted against time, the initial slope obtained is commonly referred to as the clearance, usually expressed in units of L/cm^2 · sec, or apparent permeability coefficient (Pe), in units of cm/sec (7). This quantity can be conceived as a volume of fresh medium "transported" to the donor compartment per unit cell surface area and unit time. Mass transported at 37°C across the MDCK cell monolayer is shown in Fig. 1 for a series of short-chain carboxylic acids. On the same graph, we also indicated the scale of the percentage of total solute

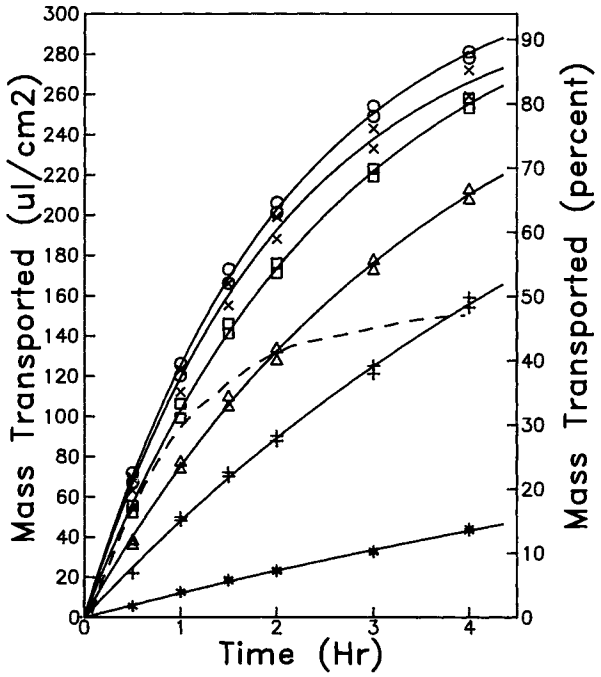

Fig. 1. Mass transported across a monolayer of MDCK cells at 37°C. The radioactive solute was placed in the 1.5-ml apical compartment and transport was measured by monitoring the appearance of radioactivity in the 2.6-ml basal compartment. The initial concentration of the ^{14}C-labeled acid was 10 μM, and that of the unlabeled carrier acid 2.5 mM. (○) OA; (x) HA; (□) VA; (△) BA; (‡) PA; (*) AA. The dashed line represents the transport of OA without the unlabeled acid. The solid lines are theoretical first-order curves calculated using the parameters obtained by nonlinear least-squares analysis (8) of the experimental points.

transported for comparative purposes. The apical-to-basal transport was studied by monitoring the appearance of radioactivity in the basal compartment when 10 μM [^{14}C]RCOOH and 2.5 mM cold RCOOH were placed initially in the apical donor compartment. In all cases, each symbol represents the average of triplicate determinations of radioactivity present in the basal side of a given cell monolayer. Thus the total number of the cell monolayer used for the data in Fig. 1 is 12. Such experiments were repeated numerous times, resulting in essentially identical data.

The transport of all compounds tested obeyed pure first-order kinetics. The experimental data were analyzed by a nonlinear least-squares fit (8) to the equation.

$$B = B_\infty(1 - e^{-kt}) \tag{1}$$

where B and B_∞ are the quantity of a compound found in the basal compartment at time = t and ∞, respectively, and k is the apparent first-order rate constant. The parameters B_∞ and k thus obtained were then used to construct the theoretical curve shown in Fig. 1. The excellent agreement between the calculated curves and the experimental points then supports the conclusion that the transport is pseudo first-order with respect to the acid in the donor compartment. Most notable is the absence of any induction period and the lack of accumulation of any measurable quantity of acid in the cell layer. On the basis of these observations one can safely interpret the data in terms of a diffusion model with the transported solute at a steady state in the barrier compartment, which consists of the cell layer and the membrane filter.

The dashed line in Fig. 1 represents the transport of OA in the absence of the cold compound. Several lines of evidence show that the apparent decrease in OA transport in the absence of cold compound is due to the catabolism of OA. First, we were able to trap [^{14}C]CO_2 in 0.1 N NaOH from the head space of cell monolayers. Second, the transport of AA and PA was hardly affected by cold compound (experimental data not shown here). It thus appeared that β-oxidation had taken place, with [^{14}C]acetyl-CoA breaking down to [^{14}C]CO_2 via the TCA cycle (5). Third, the mass balance at t = 4 hr, as measured by the radioactivity present, was only about 65% of the initial value when there was no excess OA; typically 3% from the apical medium, 14% from the cell layer, and 47% from the basal side. In contrast, the mass balance remained almost 100% throughout the experiment when a large excess of OA was present. Finally, a GC/MS analysis with single-ion monitoring at m/e 60 showed that, in the presence of unlabeled compound, the radioactivity in the acceptor compartment was associated with intact OA only. A similar analysis indicated that only about 10% of the radioactivity in the acceptor compartment was from intact OA at t = 4 hr when 10 μM [^{14}C]OA alone was employed.

As pointed out above, the initial slope of each transport profile in Fig. 1 is equal to Pe. This together with Eq. (1),

$$\text{Pe} = \left[\frac{dB}{dt}\right]_{t=0} = kB_\infty \tag{2}$$

The values of Pe for six carboxylic acids we studied are summarized in Table I along with k values. The standard deviation (SD) of a given Pe value was estimated from (SD for k) × B_∞ + (SD for B_∞) × k and is also listed in Table I.

For a solute that must diffuse across an "unstirred aqueous layer" and a membrane (cell monolayer in the present case),

$$\text{Pe} = \frac{P_m \cdot P_{aq}}{P_m + P_{aq}} \tag{3}$$

where P_{aq} and P_m are permeability coefficients of the solute in the aqueous phase and in the membrane, respectively (9).

Table I. Pseudo First-Order Rate Constant (k) and Apparent Permeability Coefficient (Pe) for Transport of a Series of Aliphatic Carboxylic Acids Across the MDCK Cell Monolayer at 37°C and pH 7.4 with Minimum Disturbance in Hydrodynamics[a]

Acid	(k ± SD) × 10^5 (sec^{-1})	(Pe ± SD) × 10^5 ($cm \cdot sec^{-1}$)
Acetic	2.11 ± 0.53	0.348 ± 0.163
Propionic	4.02 ± 0.46	1.42 ± 0.29
Butyric	7.35 ± 0.46	2.37 ± 0.24
Valeric	10.4 ± 0.41	3.42 ± 0.21
Heptanoic	13.3 ± 0.78	4.17 ± 0.37
Octanoic	13.3 ± 0.40	4.37 ± 0.20

[a] Values of k and standard deviations (SD) were obtained by the damping Gauss–Newton method of nonlinear least-squares fit (8) of the data shown in Fig. 1 to Eq. (1).

The latter is proportional to the solute concentration in the membrane, which is in turn determined by the partition coefficient (K) of the solute between the membrane and the aqueous phase. Throughout the present study, the initial concentration of all carboxylic acids tested was constant at 2.5 mM. Thus,

$$P_m = \alpha K \tag{4}$$

For a series of carboxylic acids containing n number of carbons, the free energy associated with the transfer of 1 mole from the aqueous phase to the membrane can be separated into that from $-CH_2-(\beta)$ and that from -COOH-group (γ) transfer.

$$\Delta G = \beta(n - 1) + \gamma = -RT \ln K \tag{5}$$

Substitution of K from Eq. (5) to Eq. (4) results in an expression of P_m as a function of β and γ. Substitution of the latter to Eq. (3) leads to Eq. (6).

$$\mathrm{Pe} = P_{aq} \cdot \alpha \cdot \exp\left(\frac{-\beta}{RT} n + \frac{\beta - \gamma}{RT}\right) \Big/ P_{aq} + \alpha \cdot \exp\left(\frac{-\beta}{RT} n + \frac{\beta - \gamma}{RT}\right) \tag{6}$$

Those six Pe values listed in Table I were fitted to Eq. (6) using a nonlinear least-squares method (8) to obtain four unknowns; P_{aq}, α, β, and γ. These parameters thus estimated were then used to construct the curve shown in Fig. 2. The value of β was found to be -0.678 ± 0.089 kcal/mol, which is almost identical to the free energy of transfer of 1 mole of $-CH_2-$ from water to n-octanol, -0.68 kcal/mol (10), indicating that the latter system is indeed a good model for $-CH_2$-group transfer to the cell membrane. In theory, γ should be the energy associated with transfer of -COOH groups at pH 7.4. In the present study, however, a large standard deviation, as much as 30% of the estimate, precludes any further discussion. This large error in the estimation of γ is primarily because of the large deviations seen with AA and PA from the theoretical curve (see Fig. 1). Note that the relative contribution of a -COOH group to the estimation of γ would be largest in AA in our studies.

The good agreement shown in Fig. 2 between experimentally determined Pe values and Eq. (6) supports a gradual change in transport mechanism as the solute changes from AA to OA, as interpreted earlier (9). In essence, as lipophilicity increases from AA to OA, partitioning onto and diffusion within the cell membrane becomes more facilitated, resulting in an aqueous boundary-controlled rate-limiting step. That is, the small increase in Pe from HA to OA compared with that from AA to PA is attributed to the fact that for the former two acids, diffusion through the unstirred aqueous layer is the major barrier of transfer. The effective thickness (h) of this boundary layer can be estimated from $h = D/\mathrm{Pe}$, where D is the aqueous diffusion coefficient of OA. If we assume D to be equal to that of n-octanol, 7.5×10^{-6} cm^2/sec (9), it becomes about 0.20 cm for the present system.

System Characterization

In the experiments shown in Fig. 1 no special precautions were taken to optimize the hydrodynamics of the system. In the case of HA, additional experiments were carried out at room temperature (22.5 ± 1°C) to study the effect of stirring on the rate of transfer. Without stirring, the only disturbance of the aqueous phases was transfer of a Transwell with a cell monolayer to the next well or replacing the apical medium with fresh HBSS at a given time. With stirring, a six-well plate was continuously swirled on a cell rocker and was interrupted only for sampling. As shown in Fig. 3, the swirling motion indeed accelerated the transport of HA across the cell layer in both directions. Also to be noted is that, in either case, the initial transport rate, i.e., apparent permeability, was identical for both transport directions. A similar experiment was run with OA which re-

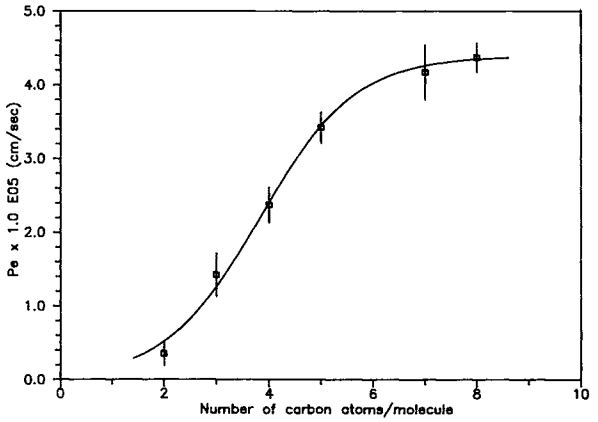

Fig. 2. Apparent permeability coefficients of six carboxylic acids in the apical-to-basal transport across the MDCK cell monolayer at 37°C as a function of the number of carbon atoms in the solute. Vertical bars represent one standard deviation resulted from the curve fitting of the data in Fig. 1. The solid line was generated from Eq. (6) using six Pe values listed in Table I. The curve fitting was carried out by means of a nonlinear least-squares analysis (8).

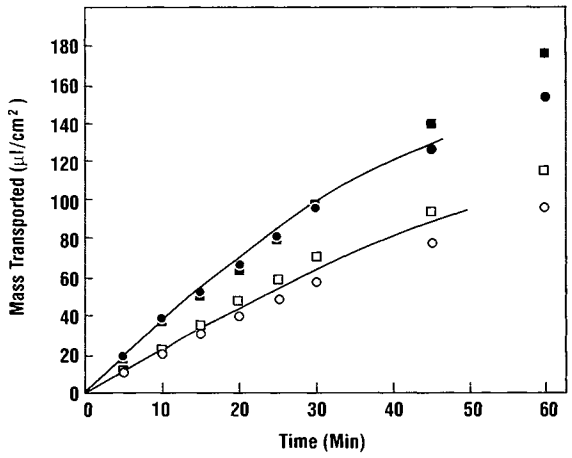

Fig. 3. Apical-to-basolateral (circles) and basolateral-to-apical (squares) transport at room temperature of [^{14}C]HA in the presence of a large excess of cold HA across the MDCK cell monolayer with (filled symbols) and without (open symbols) agitation. Each point represents the average of triplicate determinations using three separate cell layers. Variation within three determinations was very small; it seldom exceeded 2% of the average value.

sulted in an essentially identical effect of hydrodynamics on the transport.

For the transport of PA and OA, we also monitored the time course of the radioactivity in each of the three compartments. In this protocol, at each time point, one MDCK cell monolayer was sacrificed for each determination. Percentage radioactivity found in each compartment for a 90-min period is summarized in Table II. In both cases, the mass balance was fairly well maintained throughout the experiments and a small but measurable amount of the solute was retained in the cell monolayer. Although less than 1.5% for PA and 0.87% for OA was retained in the cell layer for the 90-min period, this quantity is significant in terms of concentration because of the extremely small pool volume. The total cell volume can be crudely estimated in two ways. Earlier we reported that the thickness of the MDCK monolayer at confluence is about 7 μm (1) and thus the volume in our system would be $7 \times 10^{-4} \times 4.71 = 3.3 \times 10^{-3}$ ml. Alternatively, the volume of the MDCK cell was reported to be 1170–1520 μm^3 (11) and from the cell density at confluence, 4×10^5 cells/cm^2 (1), we obtain 2.5×10^{-3} ml. That is, the total cell volume of 4.71 cm^2 of the MDCK cell monolayer is estimated to be about 3 μl. Even if we assume that PA and OA in the cell layer are distributed homogeneously, throughout the experiment their concentration would be greater in the cell layer, which was continuously in contact with the receiving compartment under a sink condition, that in the donor compartment.

Effects of Albumin and EGTA

In our preliminary studies using equilibrium dialysis technique, it was found that at HSA concentrations greater than 0.3%, more than 90% of 10 μ*M* OA was albumin-bound. Since proteins are transported extremely slowly, the effect of albumin on the OA transport across the MDCK cell monolayer was rather significant. When the transport of 10 μ*M* OA was studied, the effect of the initial 0.1% albumin was much greater than that observed with the same 0.1% increment of albumin from 0.4 to 0.5%. At $t = 4$ hr, the amount of OA transported from the apical to the basal side was 47, 26, and 23% in the presence of 0, 0.1, and 0.5% HSA in the donor side, respectively. When 0.5% HSA was placed in the acceptor compartment only, very little change in the rate of transport was observed. When 0.5% HSA was placed in both donor and receiver compartments, its effect was identical to that of albumin present only in the donor compartment.

The presence of EGTA at low concentrations in Ca^{2+}/Mg^{2+}-free HBSS is known to cause opening of the intercellular tight junctions of the MDCK cell monolayer (6,12). Under such conditions, as shown in Fig. 4, the transport of a fluid-phase marker LY was extremely fast, indicating that the transport of LY occurs primarily via the paracellular shunt pathway (1). PA transport was also significantly enhanced when the paracellular route opened up, but the increase was less than in the case of LY. Most interestingly, as shown by the dashed line in Fig. 4, opening the tight junctions did not affect the transport of OA. This then indicates that the transport of OA occurs primarily through diffusion in the cell membrane.

The transport rate of HSA across the MDCK cell layer was estimated from that of [^{125}I]BSA. As expected, the latter was found to be extremely slow; less than 0.05% of the amount present was transported in 4 hr when a 0.5% solution of BSA was placed in the apical side at $t = 0$. In 0.1 m*M* EGTA, however, as much as 12% of the BSA was transported in 4 hr; the BSA transport was almost linear after an

Table II. Percentage Radioactivity Recovered During Apical-to-Basal Transport[a]

	Time (min)					
	5	10	20	35	60	90
	Propionic acid					
Donor	101.0	99.0	92.9	87.7	76.8	65.4
Cell layer	0.2	0.3	0.6	1.0	1.3	1.5
Receiver	1.6	2.6	5.2	11.7	19.6	30.5
Total recovery	102.8	101.9	98.7	100.4	97.7	97.4
	Octanoic acid					
Donor	91.2	86.8	80.7	73.0	58.7	46.8
Cell layer	0.30	0.31	0.44	0.58	0.72	0.87
Receiver	5.3	9.7	16.6	24.6	38.0	50.1
Total recovery	96.8	96.8	97.7	98.2	97.4	97.8

[a] The radioactivity was from 10 μ*M* [^{14}C]RCOOH in the presence of 0.1 m*M* propionic acid or 1.0 m*M* octanoic acid. All numbers are averages of duplicate (for PA) or triplicate (for OA) experiments.

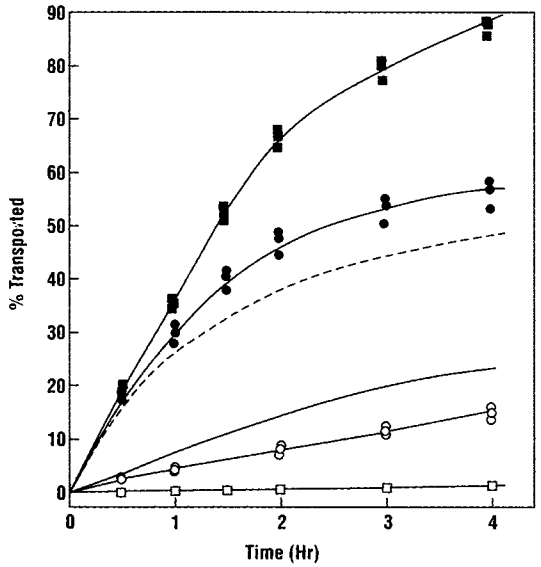

Fig. 4. Apical-to-basal transport of LY (squares) and PA (circles) across the MDCK cell monolayer at 37°C in normal HBSS (open symbols) and in Ca^{2+}/Mg^{2+}-free HBSS containing 0.1 m*M* EGTA (filled symbols). Identical transport rates were observed for OA regardless of EGTA, both in the absence (dashed line) and in the presence (solid line without symbols) of 0.5% HSA in the donor compartment. Each symbol represents an independent determination on a separate cell monolayer but the average of triplicate analysis of permeants, either radioactivity or fluorescence intensity. In the case of LY, only the average of three independent determinations is presented. The dashed line in this figure should be identical to that in Fig. 1.

initial lag time of about 60 min (raw data not shown). In the presence of 0.5% HSA, over 95% of OA exists as bound to HSA when the total OA concentration is 10 μM, exclusively from radiolabeled OA. As pointed out earlier, at the 10 μM level of OA, its transport across the cell monolayer is subject to a significant catabolism. Based on the significant paracellular leakage of albumin when tight junctions remain opened and the strong binding of OA to albumin, we had anticipated that OA transport would be significantly enhanced if albumin is present not only as a "carrier" but also as a "protector" of OA from catabolism when the transport is monitored in Ca^{2+}/Mg^{2+}-free HSBB containing EGTA. Enhancement of the transport should have been at least 10% greater than in the absence of HSA over a 4-hr period. Our experimental reproducibility was such that we should have been able to detect such a difference in magnitude (see, for example, the transport profile of VA, HA, and OA in Fig. 1). Contrary to our expectation, OA transport in the presence of 0.5% HSA was not affected at all by EGTA in Ca^{2+}/Mg^{2+}-free HBSS (solid line in Fig. 4). This observation is most likely due to preferential partitioning of free OA onto and diffusion in the cell membrane rather than paracellular transport of OA–HSA complex. This set of observations emphatically illustrates how negligible is the paracellular route of transport for a lipophilic substance such as OA, even when most of OA is in the anionic form at pH 7.4.

Finally, our results shed some light on the details of transcellular transport, as observed with HA and OA. Two additional observations sugggest that the actual path of the transported molecules is limited to the cell membrane and its immediate neighborhood. First, the rate of transport is independent of direction. All transporting epithelia composed of polarized cells demonstrate directional ion flux by means of various ion channels (13). In the present study, the net flux occurs in carboxylate anion form. Since its counter ions such as Na^+, Ca^{2+}, Mg^{2+}, K^+, etc., are subject to directional transport, one would expect some directionality across the highly polarized MDCK cells, if diffusion within the cytoplasm were a major part of the transport process. Second, the initial rate of transport of OA is exactly the same in the presence and absence of cold carrier, and this in spite of the fact that in the absence of carrier OA about one-third of OA is catabolized by the cell (Fig. 1). If the major path of OA were through the cytoplasm, then the catabolic pathway would branch out from the transport pathway and thereby would decrease the rate of transfer by about one-third. This is patently not the case. We then should like to conclude that the catabolic uptake branches out of the transport pathway at an earlier stage, most probably at the pool of OA dissolved in the membrane.

In the apical-to-basal transport, HA molecules would diffuse through the unstirred aqueous boundary layer, partition onto and diffuse laterally in the apical cell membrane, desorb to surrounding HBSS medium in 3-μm pores in the synthetic membrane, and finally, diffuse out into the bulk phase after passing through another unstirred layer. The process is schematically presented in Fig. 5. In the basal-to-apical transport, HA molecules should first find 3-μm pores in the polycarbonate membrane. Approximately 14% of the total surface area is from the pores (14). The subsequent steps should be much the same as in the apical-to-basal processes except that they are in a reverse order. Very little is known about the molecular movement in each step. The permeability analysis presented earlier simply indicates that the diffusion in an aqueous phase, possibly both at the apical cell membrane and at the bottom side of the polycarbonate membrane, is an important rate-controlling step. The diffusion-controlled transport is further substantiated by the identical Pe observed for both directions of transport. Finally, from the temperature dependence of Pe for the apical-to-basal transport of OA without agitation, 3.72×10^{-5} cm/sec at 37°C (Table I) and 2.78×10^{-5} cm/sec at 22.5°C determined in a separate experiment, we obtained an apparent activation energy of 3.7 kcal/mol. Once again, this is in good agreement with a diffusional process of low molecular weight compounds in aqueous medium (7).

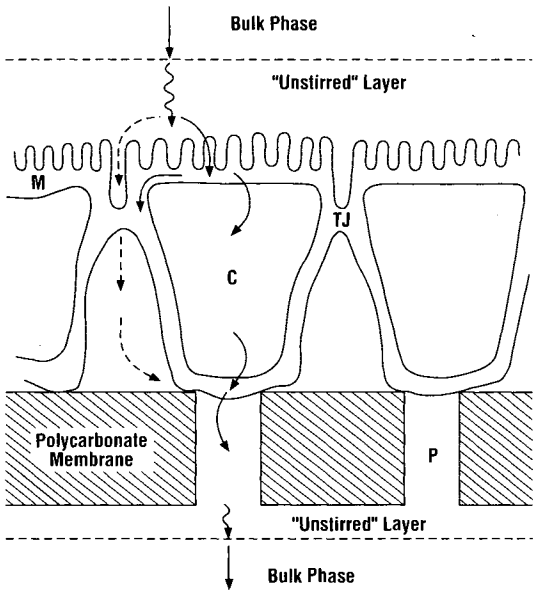

Fig. 5. A schematic diagram for the apical-to-basolateral transport. In the transcellular route (solid lines), solutes such as OA would enter the cell membrane (M) after diffusing through a rate-limiting "unstirred" layer (dotted lines), followed by either desorption to cytoplasm (C) or lateral diffusion in M, and finally leave M for pore space (P) in the polycarbonate membrane. In the paracellular route (dotted lines), solutes such as AA would pass through the tight junctions (TJ) and lateral space.

CONCLUSION

The present study employed the MDCK cell monolayer as a model barrier in assessing the effect of chain length, and thus lipophilicity, on the cellular transport of a series of simple carboxylic acids. All our results are in agreement with those obtained with an animal gut perfusion model (9). In the light of our earlier work, where we studied the transport of polar substances with a wide range of molecular size (1), the present study promises a wide range of applications of this cell system for drug development. It has already been applied to investigating a potential mechanism by which the so-called GI absorption adjuvants work (12) and to developing a chemotaxis model in which neutrophil-mediated extravasation is studied *in vitro* (15). We feel that the system developed in this study is ideally suited for screening a series

of new chemical entities, especially drug candidates, for optimum transport properties.

ACKNOWLEDGMENTS

The authors acknowledge helpful discussions with Dr. Norman Ho and the GC/MS data made available by Mr. C. L. Barsuhn, both from the PR&D Division, The Upjohn Company. A.A. expresses a special gratitude to the following Upjohn personnel: Ms. Beth Whitted and Mrs. Char Martin for their hospitality during his stay at the Upjohn Company and Mr. Dosh Jackson for the opportunity to carry out the present study.

REFERENCES

1. M. J. Cho, D. P. Thompson, C. T. Cramer, T. J. Vidmar, and J. F. Scieszka. *Pharm. Res.* 6:71–77 (1989).
2. V. L. Sallee and J. M. Dietschy. *J. Lip. Res.* 14:475–484 (1973).
3. N. F. H. Ho and W. I. Higuchi. *J. Pharm. Sci.* 60:537–541 (1971).
4. A. A. Spector. *J. Lip. Res.* 16:165–179 (1975).
5. A. L. Lehninger. *Biochemistry,* Worth, New York, 1978, pp. 543–558.
6. A. Martinez-Palomo, I. Meza, G. Beaty, and M. Cereijido. *J. Cell. Biol.* 87:736–745 (1980).
7. G. L. Flynn, S. H. Yalkowsky, and T. J. Roseman. *J. Pharm. Sci.* 63:479–510 (1974).
8. K. Yamaoka, T. Tanigawara, T. Nakagawa, and T. Uno. *J. Pharm. Dyn.* 4:879–885 (1981).
9. N. F. H. Ho, J. Y. Park, W. Morozowich, and W. I. Higuchi. In E. B. Roche (ed.), *Design of Pharmaceutical Properties Through Prodrugs and Analogs,* Am. Pharm. Assoc., Acad. Pharm. Sci., Washington, DC, 1977, pp. 136–227.
10. A. Leo, C. Hansch, and D. Elkins. *Chem. Rev.* 71:526–616 (1971).
11. C. H. Von Bonsdorff, S. D. Fuller, and K. Simons. *EMBO J.* 4:2781–2792 (1985).
12. M. J. Cho, J. F. Scieszka, and P. S. Burton. *Int. J. Pharm.* 52: 79–81 (1989).
13. S. G. Schultz. *Basic Principles of Membrane Transport,* Cambridge University Press, UK, 1980.
14. *Nucleopore Catalog,* Nucleopore Corp., Pleasanton, CA, 1984, p. 39.
15. M. J. Cho, J. F. Scieszka, C. T. Cramer, D. P. Thompson, and T. J. Vidmar. *Pharm. Res.* 6:78–84 (1989).